

GLOBAL CHARACTERIZATION OF ROSSBY WAVES AT SEVERAL SPECTRAL BANDS

Paulo S. Polito¹ and W. Timothy Liu²

¹ Earth Observation Department
INPE - National Institute for Space Research, Brazil

² Jet Propulsion Laboratory
California Institute of Technology

INTRODUCTION

Rossby waves are the ocean's response to large scale perturbations, based on conservation of potential vorticity. Typically these waves are $\sim 1,000$ – $10,000$ km long, have a period of months to years and cause a surface displacement of ~ 1 – 10 cm.

As a first approximation the ocean behaves as a two-layer system with the vertical displacement of the interface induced by Rossby waves. These vertical displacements are ~ 10 – 100 m.

These long, baroclinic waves are non-dispersive and transport energy westward to help maintain the mid-latitude gyres and to intensify the western boundary currents. The energy and the phase propagate westward at the same speed with a typical magnitude of 1– 100 km/day.

The TOPEX/Poseidon altimeter (T/P) provided for the first time a long global time series of the sea surface height anomaly (η). Recent results based on T/P from [Chelton and Schlax(1996)] (CS) and [Zang and Wunsch(1999)] (ZW) raised an interesting debate over the validity of the standard linear theory to estimate the Rossby wave phase speed.

In this study a series of finite impulse response (FIR) filters are used to separate the T/P η into several dynamical components. The phase speed c_p , period T , wavelength L , fractional variance V , amplitude A , and signal-to-noise ratio S/N are estimated.

The same technique has been successfully applied to compare heat storage from T/P and in situ data in [Polito et al.(2000)] since the effect of salinity on η is small [Sato et al.(1999)]. A modified Radon transform technique [Polito and Cornillon(1997)] was used to estimate c_p .

METHODS

The bin-averaged η data from the WOCE dataset (JPL/PODAAC) has the 8-year mean (93–00) removed and are bicubically interpolated in space to a $1^\circ \times 1^\circ$ grid. Maps of $\eta_o(x, y)$ for the Pacific, Atlantic, and Indian basins are converted to zonal-temporal diagrams of $\eta_o(x, t)$, one per latitude.

The η_o is decomposed through FIR filters into:

$$\eta_o = \eta_t + \eta_{24} + \eta_{12} + \eta_6 + \eta_3 + \eta_1 + \eta_K + \eta_E + \eta_r. \quad (1)$$

- η_t is the non-propagating, **basin-scale** signal dominated by seasonality and ENSO.
- η_{24} to η_3 are long first-mode **Rossby waves** with approximate periods of **24, 12, 6, and 3 months**.
- η_1 has a period of **1.5 months** and is dominated by **tropical instability waves (TIWs)**.
- η_K is present only in the equatorial region as a fast eastward propagating semiannual signal identified as **Kelvin waves**.
- η_E includes **meso-scale eddies** and other features that cannot be identified as any of the above.
- η_r is dominated by small scale, high frequency residual.

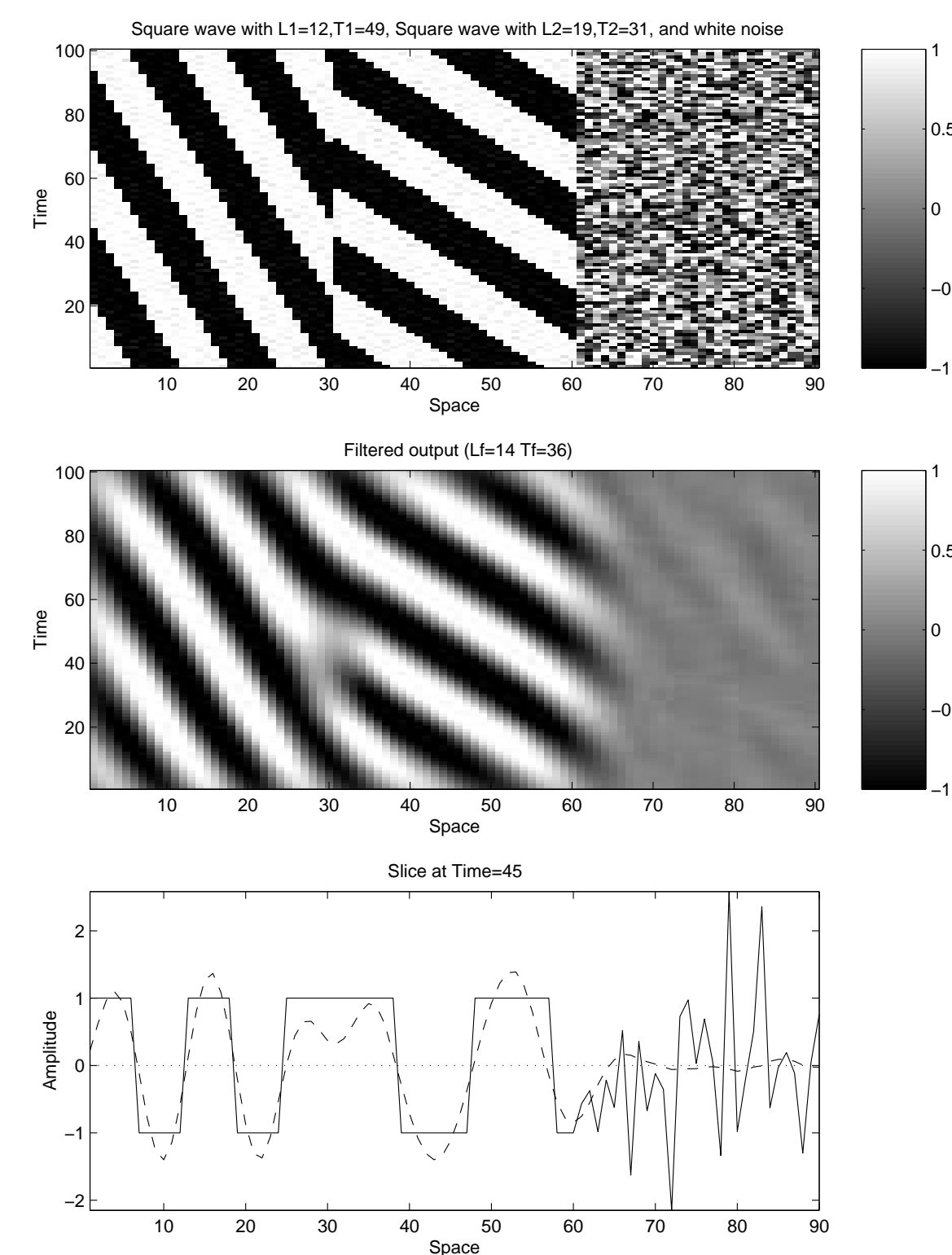


Figure 1: (Top) Input data with two square waves characterized by L_1 , T_1 , L_2 and T_2 , and white noise. (Middle) Application of the filter characterized by L_f and T_f preserves the original phase, period, wavelength, and phase speed. (Bottom) Results for Time=45 with the original data (-) and the filtered data (-).

Figure 1 shows an example of the filter performance. Two square-waves and a random noise field form a single matrix. This matrix is filtered with one single FIR filter similar to the one used for the T/P

data. The filter period, wavelength, and phase speed are slightly different from those used to build the input data. This test demonstrates that:

- filtering **does not change** the c_p , T , L , or A of the original signal.
- even when the filter does **not exactly** match the wave characteristics, its performance is **acceptable** (i.e. it has a finite bandwidth).
- the filter **does not create signals** from noise,
- no particular wave form** is assumed or enforced.

RESULTS

A series of **FIR filters** is applied to η_o to obtain the components indicated in Equation 1 for all basins and latitudes.

Figure 2 shows the filtered fields and the average c_p at 28.5°N in the Pacific. The dash-dotted lines represent the mean phase speed as are **aligned, in average, with the propagation patterns**.

In Figure 3 the wave regimes that characterize the equatorial Pacific are shown. The basin-scale component η_t is dominated by ENSO which also modulates the η_1 signal, associated with tropical instability waves.

From the filtered components shown in Figures 2 and 3 the wave parameters for each **data block** measuring approximately T by L are estimated.

Figure 4 shows the rms amplitude of the filtered η components. The color codes are different and can be used to quantify the relative intensity of these fields.

The wave parameters are shown as a function of latitude in Figures 5, 6, and 7.

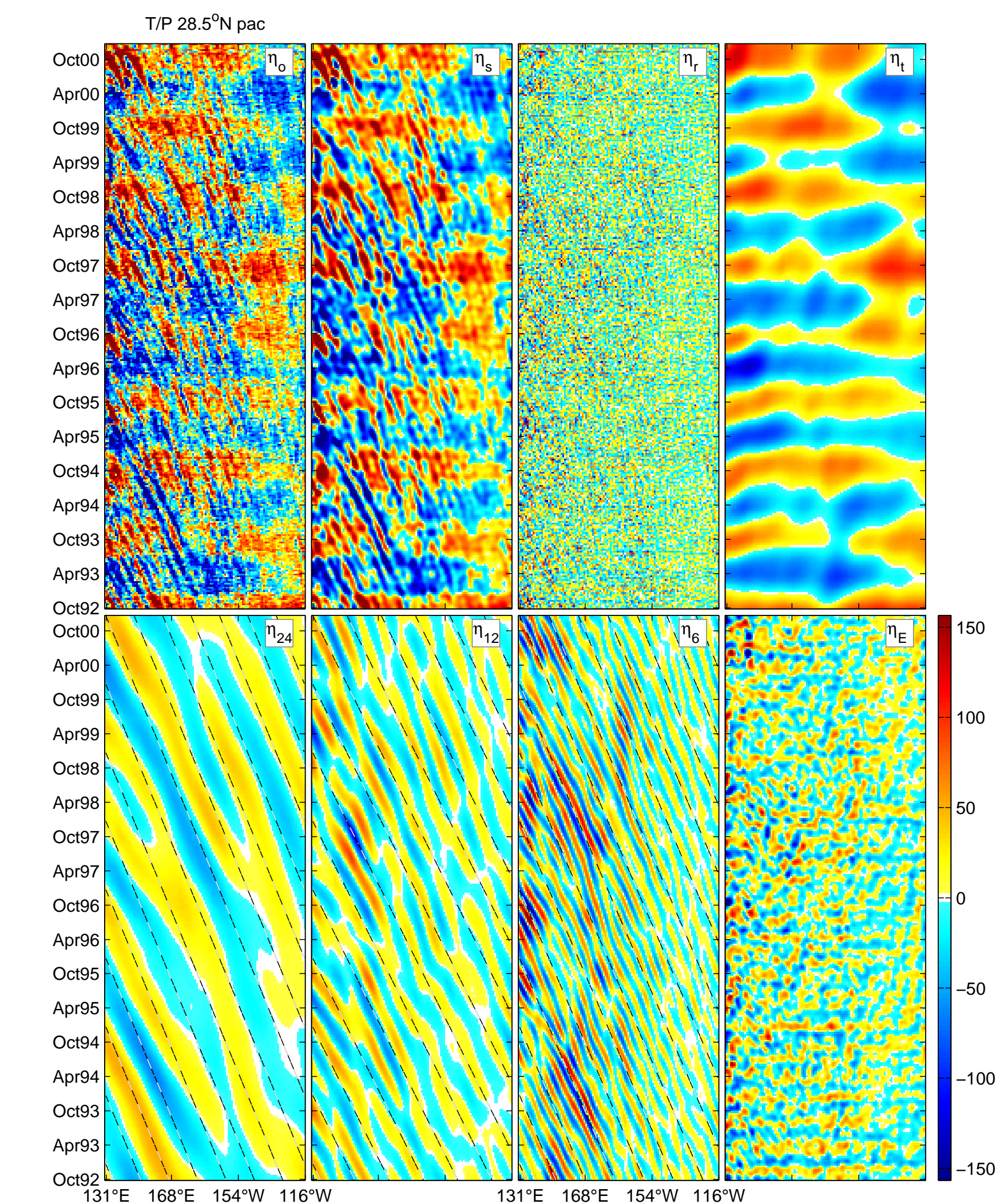


Figure 2: Original (η_o), sum of filtered (η_s), residual (η_r), and filtered sea surface height anomaly fields (η_t , η_{24} , η_{12} , η_6 , and η_3), at 28.5°N in the Pacific, in mm. Dash-dotted lines are estimates for mean zonal phase speed.

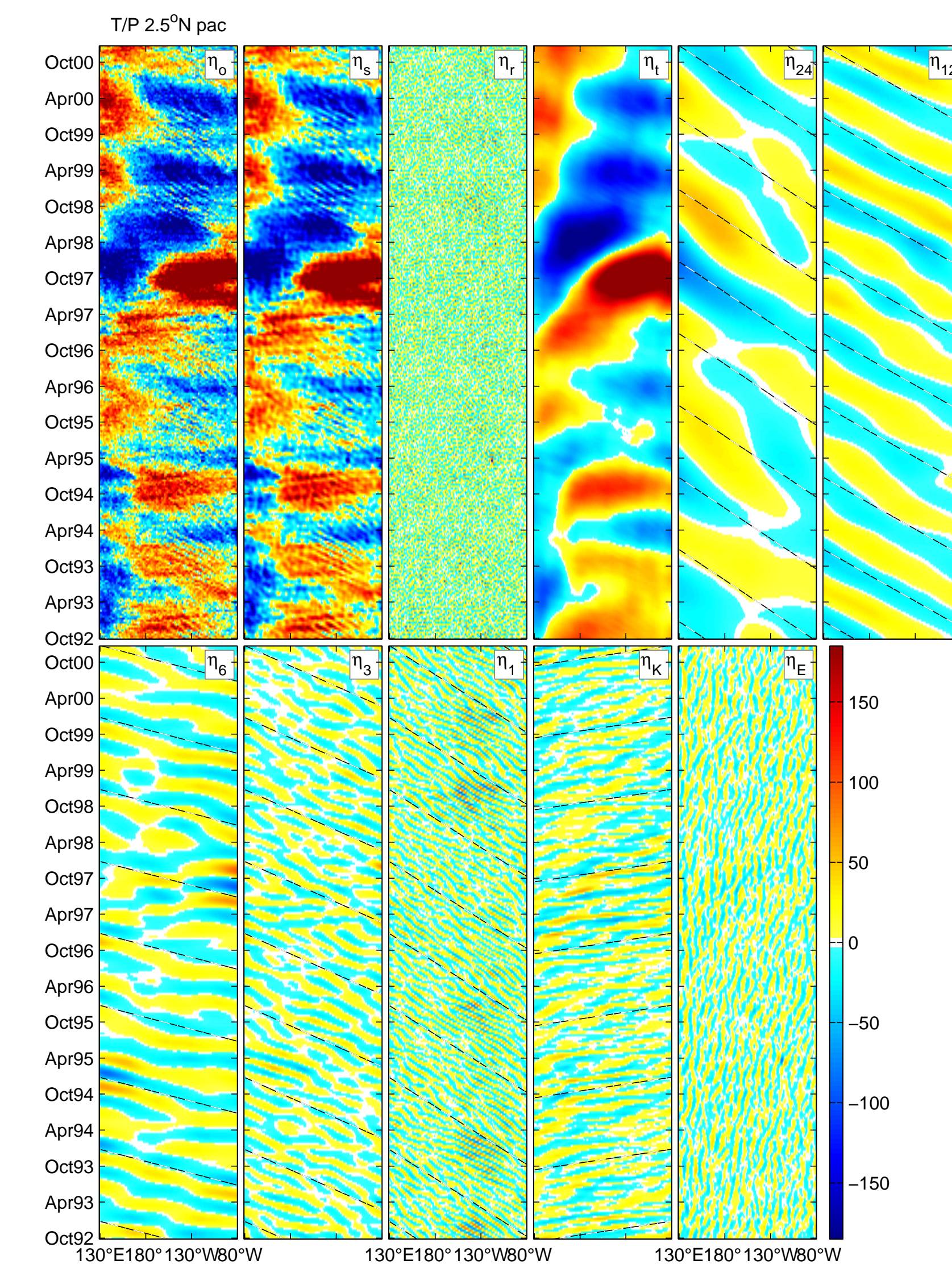


Figure 3: Similar to Figure 2 at 2.5°N in the Pacific showing the equatorial components.

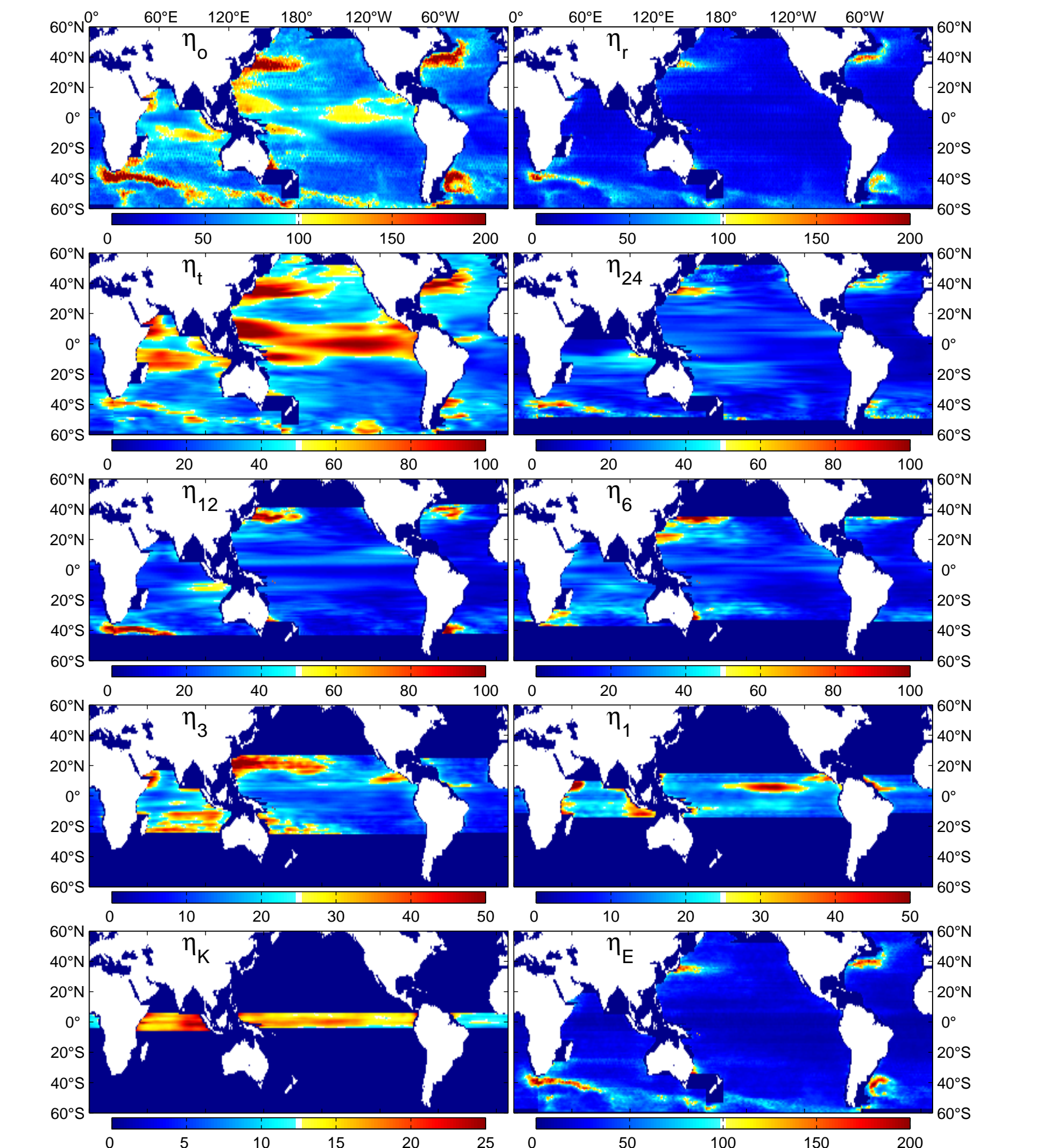


Figure 4: Rms amplitude (mm) of the filtered sea surface height components in mm, as in Equation 1. The latitudinal cut-off marks where the spatial resolution of T/P is no longer sufficient to sample the waves.

CONCLUSIONS

- Globally, the oceanic **Rossby waves behave approximately like free waves**. Our estimates of the average c_p are closer to the standard theory compared to those in CS, particularly at mid to high latitudes.
- In most cases our c_p estimates are **within the error bars of those in ZW**, including a few of their high-frequency cases that depart from the linear dispersion curve.

- There is a bias towards high values poleward of $\sim 30^\circ$ noticeable in Figures 5, 6 and 7 of $\sim 25\%$, much less than the factor of 2 from CS and less than the 50% from [Killworth et al.(1997)].
- The most important difference with respect to CS is that here the **spectral bands are treated separately**. It is possible that the remainder of the seasonal signal has biased the CS c_p estimates, which were based on the Radon transform, towards high values.

- Outside the equatorial region the c_p of the Rossby waves is indicative of the first baroclinic mode. An implication of this result is that the waves observed by the altimeter are a surface manifestation of the **vertical displacement of the main thermocline**.
- These waves change the local amount of heat stored in the water column, which surpasses that of the atmosphere by orders of magnitude. Therefore, Rossby waves have a potentially important influence on the **local climate variability**.

References

- [Chelton and Schlax(1996)] Chelton, D. B., and M. Schlax, Global observations of oceanic Rossby waves, *Science*, 272, 234–238, 1996.
- [Killworth et al.(1997)] Killworth, P. D., D. B. Chelton, and R. A. de Szoeke, The speed of observed and theoretical long extratropical planetary waves, *Journal of Physical Oceanography*, 27, 1946–1966, 1997.
- [Polito and Cornillon(1997)] Polito, P. S., and P. Cornillon, Long baroclinic Rossby waves detected by Topex/Poseidon, *Journal of Geophysical Research*, 102, 3215–3235, 1997.
- [Polito et al.(2000)] Polito, P. S., O. T. Sato, and W. T. Liu, Characterization and validation of heat storage variability from Topex/Poseidon at four oceanographic sites, *Journal of Geophysical Research*, 105(C7), 16,911–16,921, 2000.
- [Sato et al.(1999)] Sato, O. T., P. S. Polito, and W. T. Liu, The importance of in situ salinity for altimeter heat storage estimation, *Geophysical Research Letters*, 27(4), 549–551, 1999.
- [Zang and Wunsch(1999)] Zang, X., and C. Wunsch, The observed dispersion relationship for North Pacific Rossby wave motions, *Journal of Physical Oceanography*, 29, 2183–2190, 1999.

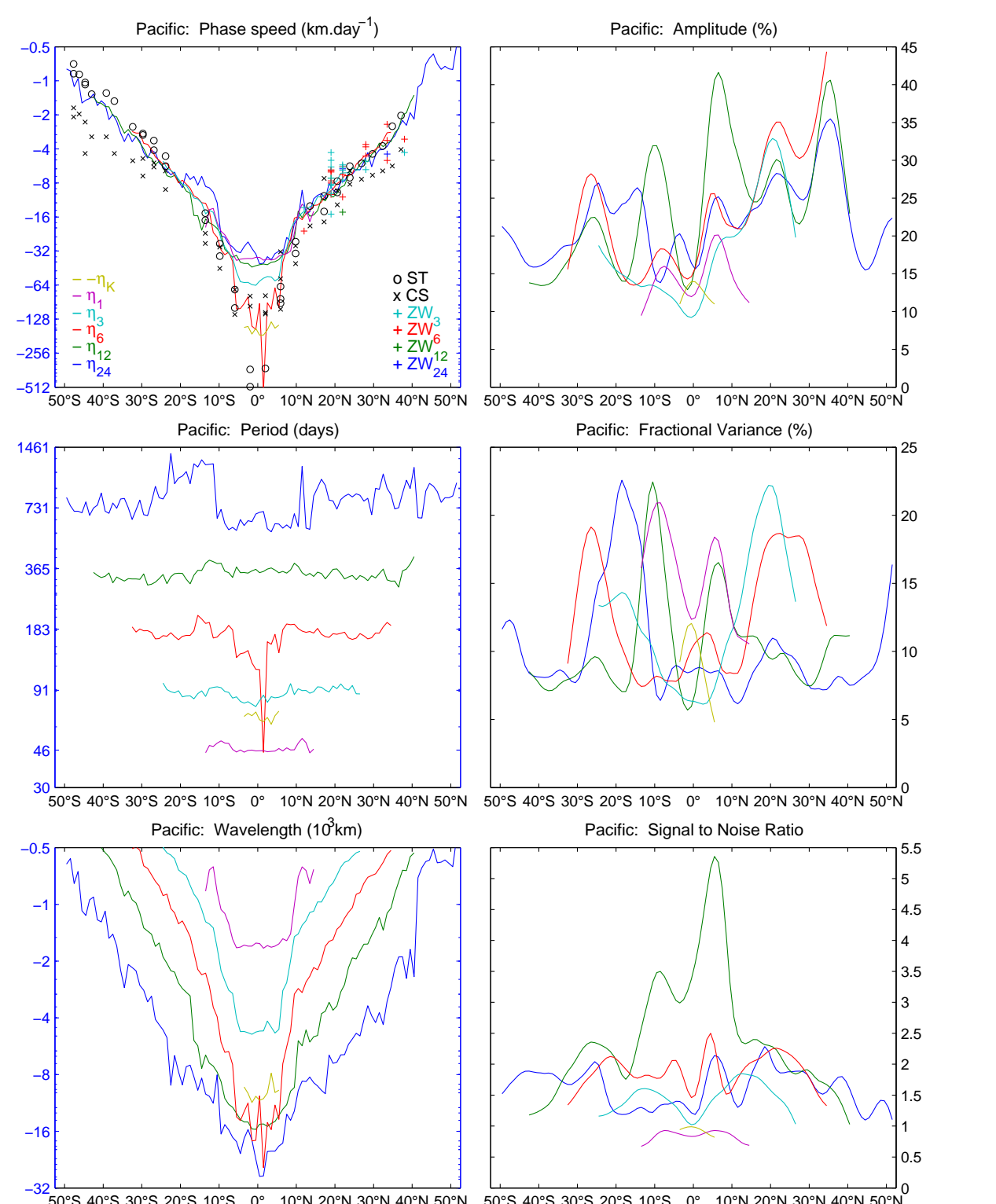


Figure 5: Mean c_p (top left), P (center left), L (bottom left), A (top right), V (center right) and S/N for the Pacific. Log (linear) axes are blue (black).

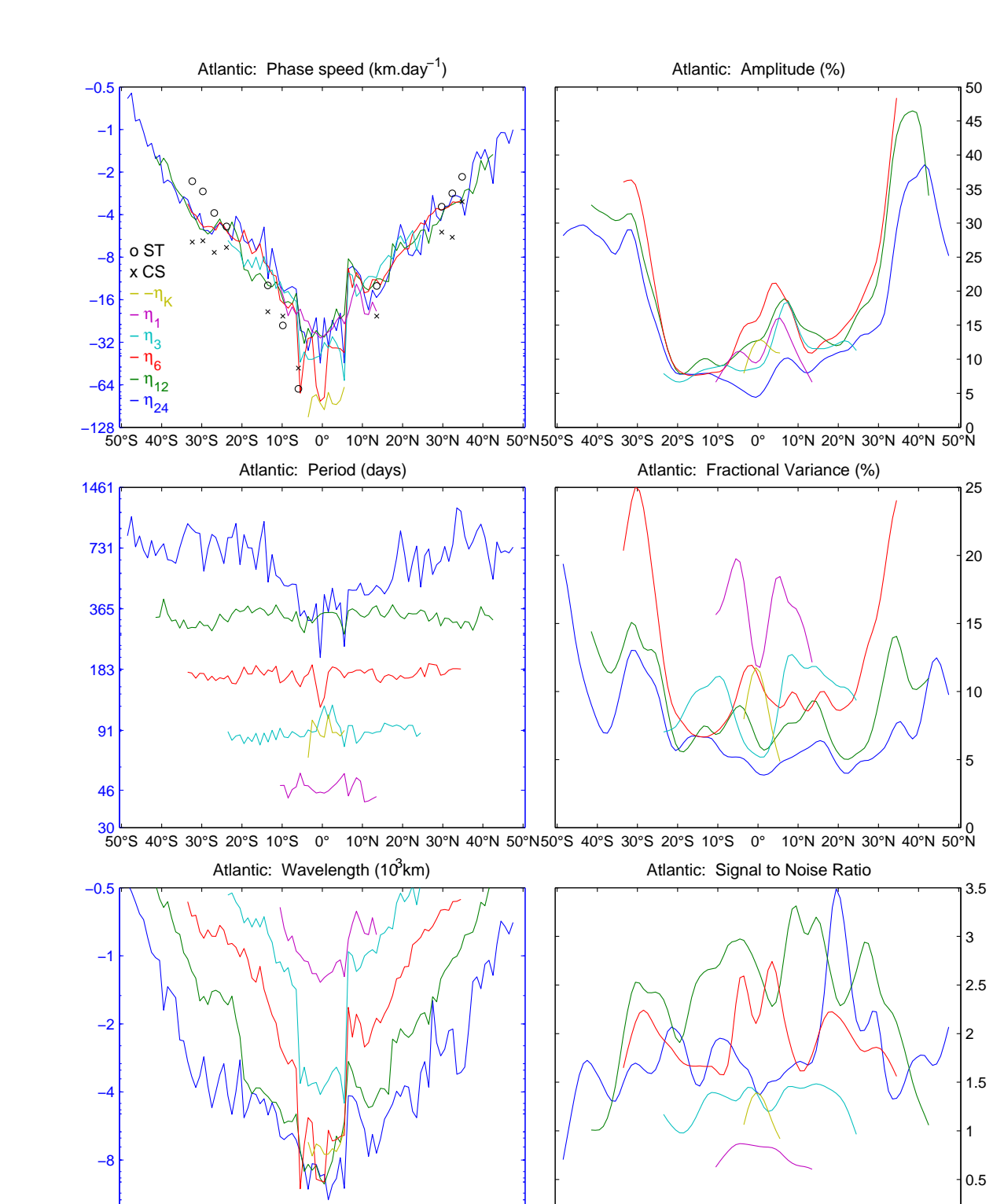


Figure 6: Similar to Figure 5 for the Atlantic ocean.

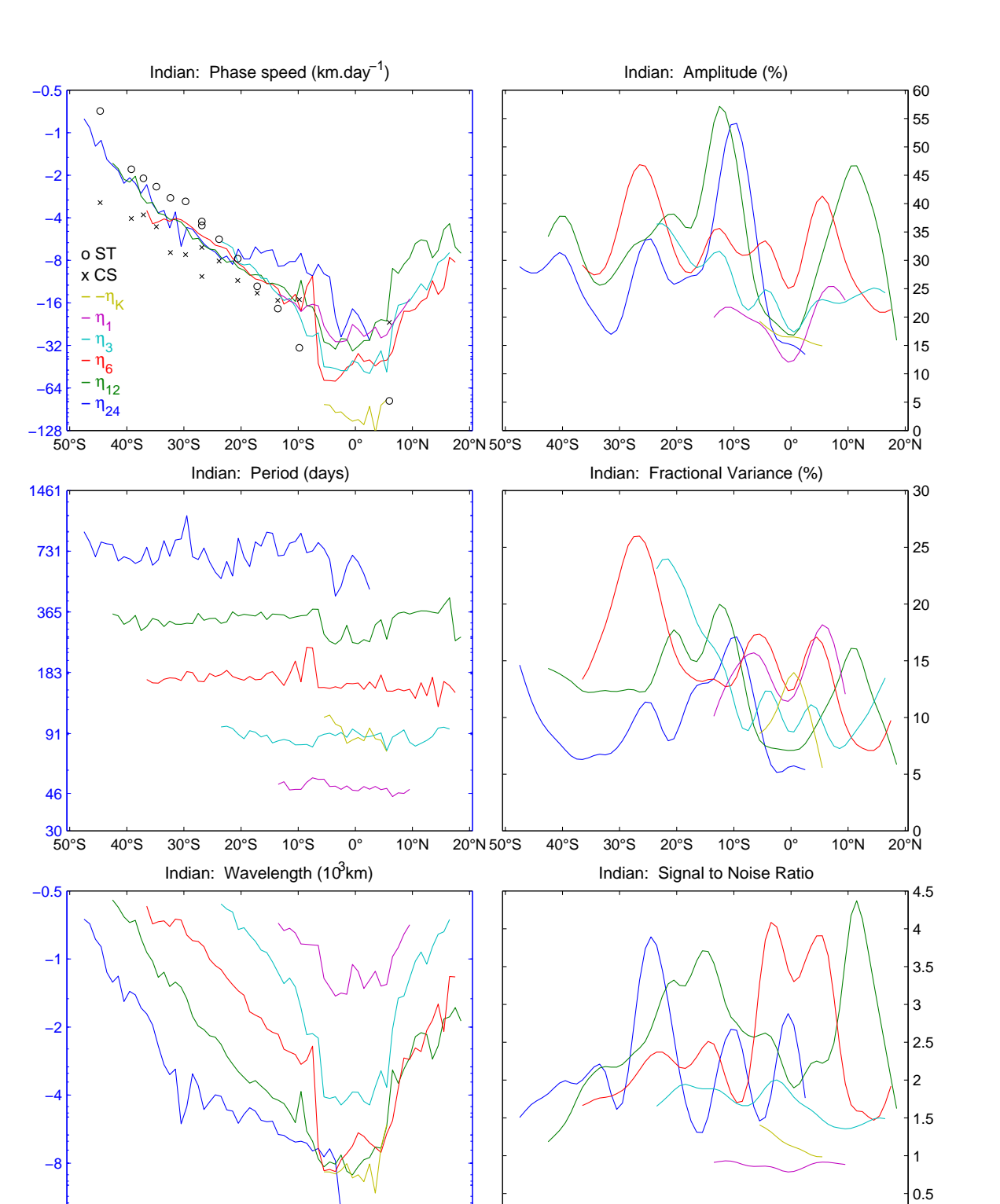


Figure 7: Similar to Figure 5 for the Indian ocean.

For more details, please e-mail us: Paulo S. Polito (polito@tid.inpe.br) W. Timothy Liu (liu@pacific.jpl.nasa.gov).